Applied and Environmental Microbiology, Mar. 2011, p. 2141–2152 Vol. 77, No. 6
0099-2240/11/$12.00 doi:10.1128/AEM.02347-10

LuxS Coexpression Enhances Yields of Recombinant Proteins in *Escherichia coli* in Part through Posttranscriptional Control of GroEL▽†

Chen-Yu Tsao,[1,2,7] Liang Wang,[2,3] Yoshifumi Hashimoto,[2] Hyunmin Yi,[2]# John C. March,[1,2]‡ Matthew P. DeLisa,[4] Thomas K. Wood,[5] James J. Valdes,[6] and William E. Bentley[1,2,7]*

Department of Chemical and Biomolecular Engineering, University of Maryland, College Park, Maryland 20742[1]; Institute of Bioscience and Biotechnology Research, University of Maryland, College Park, Maryland 20742[2]; Department of Cell Biology and Molecular Genetics, University of Maryland, College Park, Maryland 20742[3]; School of Chemical and Biomolecular Engineering, Cornell University, Ithaca, New York 14853[4]; Department of Chemical Engineering, Texas A&M University, College Station, Texas 77843[5]; U.S. Army Edgewood Chemical Biological Center, Aberdeen Proving Ground, Maryland 21010[6]; and Fischell Department of Bioengineering, University of Maryland, College Park, Maryland 20742[7]

Received 11 October 2010/Accepted 19 January 2011

Cell-to-cell communication, or quorum sensing (QS), enables cell density-dependent regulation of bacterial gene expression which can be exploited for the autonomous-signal-guided expression of recombinant proteins (C. Y. Tsao, S. Hooshangi, H. C. Wu, J. J. Valdes, and W. E. Bentley, Metab. Eng. 12:291–297, 2010). Earlier observations that the metabolic potential of *Escherichia coli* is conveyed via the QS signaling molecule autoinducer-2 (AI-2) suggested that the capacity for protein synthesis could also be affected by AI-2 signaling (M. P. DeLisa, J. J. Valdes, and W. E. Bentley, J. Bacteriol. 183:2918–2928, 2001). In this work, we found that simply adding conditioned medium containing high levels of AI-2 at the same time as inducing the synthesis of recombinant proteins doubled the yield of active product. We have hypothesized that AI-2 signaling "conditions" cells as a natural consequence of cell-to-cell communication and that this could tweak the signal transduction cascade to alter the protein synthesis landscape. We inserted *luxS* (AI-2 synthase) into vectors which cosynthesized proteins of interest (organophosphorus hydrolase [OPH], chloramphenicol acetyltransferase [CAT], or UV-variant green fluorescent protein [GFPuv]) and evaluated the protein expression in *luxS*-deficient hosts. In this way, we altered the level of *luxS* in the cells in order to "tune" the synthesis of AI-2. We found conditions in which the protein yield was dramatically increased. Further studies demonstrated coincident upregulation of the chaperone GroEL, which may have facilitated higher yields and is shown for the first time to be positively regulated at the posttranscriptional level by AI-2. This report is the first to demonstrate that the protein synthesis capacity of *E. coli* can be altered by rewiring quorum sensing circuitry.

Quorum sensing (QS) enables population density-based regulation of gene expression, whereby a single cell senses and communicates with a minimal population unit (or quorum) needed for orchestrating population behavior (12, 13, 22, 35). While there is intense interest in understanding the mechanisms of QS signal transduction, there have been few technological or commercial applications that have resulted directly from adapting or rewiring this signaling process. One of the most striking targets is in the field of metabolic engineering, where signaling modules can be constructed to alter phenotype and aid in the synthesis of recombinant gene products (30, 44, 45). For example, Bulter et al. (5) created an artificial genetic switch using acetate for modulating cell-to-cell signaling in *Escherichia coli*. Neddermann et al. (31) developed a hybrid expression system by incorporating the quorum circuitry of *Agrobacterium tumefaciens* (e.g., TraR) into a eukaryotic transcriptional controller for HeLa cells. Weber et al. (49) utilized the *Streptomyces* bacterial QS system for initiating heterologous protein expression in mammalian cell cultures and mice (human primary and mouse embryonic stem cells). Tsao et al. (45) demonstrated autoinduced heterologous protein expression in *E. coli* by rewiring the native autoinducer-2 (AI-2) signal transduction cascade.

The ability of bacteria, such as *E. coli*, to produce the AI-2 quorum signal has been attributed to the LuxS protein, a homodimeric zinc metalloenzyme originally identified in *Vibrio harveyi* (27, 41). AI-2 signal generation results from LuxS-catalyzed cleavage of *S*-ribosylhomocysteine (SRH), yielding homocysteine and 4,5-dihydroxy-2,3-pentanedione (DPD), which is cyclized into AI-2 (37, 52). The specific genes, proteins, pathways, and functions attributed to AI-2 signaling in *E. coli*, while described to be widespread (8, 10), are not fully understood and are continually emerging (1, 24, 46). For example, the genes regulated via phosphorylated AI-2 and those regulated by unphosphorylated AI-2 are different (28). Notably, important phenotypes have been attributed to AI-2 signal-

* Corresponding author. Mailing address: University of Maryland, 5115 Plant Sciences Building Number 036, College Park, MD 20742. Phone: (301) 405-4321. Fax: (301) 314-9075. E-mail: bentley@eng.umd.edu.

Present address: Department of Chemical and Biological Engineering, Tufts University, Boston, MA 02155.

‡ Present address: Department of Biological and Environmental Engineering, Cornell University, Ithaca, NY 14853.

† Supplemental material for this article may be found at http://aem.asm.org/.

▽ Published ahead of print on 28 January 2011.

TABLE 1. Bacterial strains and plasmids used in this study

Strain or plasmid	Relevant genotype or description	Source or reference
Strains		
E. coli		
W3110	K-12 strain, wild type, λ^- F^- IN(*rrnD-rrnE*)1 *rph-1s*	CGSC[a]
MDAI2	W3110 *luxS*::Tc^r W3110-derived *luxS* mutant strain	8
BL21	F^- *ompT* [*dcm*][*lon*]*hsdS*(r_B^- m_B^-)*gal*	Novagen
V. harveyi		
BB152	BB120 *luxL*::Tn*5* (AI-1^- AI-2^+) Km^r	40
BB170	BB120 *luxN*::Tn*5* (sensor 1^- sensor 2^+) Km^r	2
Plasmids		
pKK223-3	Cloning vector, Ap^r	Pharmacia Biotech
pTrcHisA,B,C	Cloning vector, Ap^r	Invitrogen
pBADHisA	Cloning vector, Ap^r	Invitrogen
pTrcHisCAT	pTrcHis derivative, Ap^r	Invitrogen
pKKluxS	pKK223-3 derivative, *luxS*$^+$ Ap^r	This study
pTO	pTrcHisA derivative, containing *opd*, Ap^r	39
pBO	pBADHisA derivative, containing *opd*, Ap^r	This study
pBOL	pBO derivative, containing *luxS* from W3110, Ap^r	This study
pBOL-LacI^q	pBO derivative, containing *luxS* from W3110 and *lacI*^{q}, Ap^r	This study
pBC	pBO derivative, containing *cat*, Ap^r	This study
pBCL	pBC derivative, containing *luxS* from W3110, Ap^r	This study
pBCL-LacI^q	pBC derivative, containing *luxS* from W3110 and *lacI*^{q}, Ap^r	This study
pTrcHisGFPuv	pTrcHisB derivative, containing GFPuv gene, Ap^r	6
pBG	pBO derivative, containing GFPuv gene, Ap^r	This study
pBGL	pBG derivative, containing *luxS* from W3110, Ap^r	This study
pBGL-LacI^q	pBG derivative, containing *luxS* from W3110 and *lacI*^{q}, Ap^r	This study
pTrcHis-LuxS	pTrcHisC derivative, containing *luxS* from W3110, Ap^r	17
pTrcHis-Pfs	pTrcHisC derivative, containing *pfs* from W3110, Ap^r	17

[a] Coli Genetic Stock Center, Yale University, New Haven, CT.

ing (e.g., virulence, biofilm formation, etc.) (11, 17). We have demonstrated that AI-2 also communicates the "metabolic potential" of *E. coli* cells, particularly when they are expressing recombinant proteins (8, 9). The signal level in the extracellular milieu decreased precipitously upon the overexpression of recombinant proteins, at a rate proportional to their rate of synthesis. This observation was independent of the protein, whether of viral, bacterial, or eukaryotic cell origin (8, 9). We subsequently hypothesized that the protein synthesis landscape (e.g., chaperone, protease, and polymerase activities) could be altered by shifting the window of quorum-dependent gene regulation through the addition of exogenous AI-2 or modulation of AI-2 production via the regulation of *luxS*.

While metabolic engineering studies often target, via complementation or mutation, the proteins or enzymes directly involved in a particular pathway of interest, such as TraR-mediated expression in eukaryotic hosts (31), an approach described here targets the native signal transduction pathway to alter the global landscape necessary for the desired objective. That is, we describe the intentional manipulation of AI-2 synthase, LuxS, in order to alter QS signaling and improve the synthesis of recombinant proteins. We have confirmed that the approach is general by testing several proteins of interest. Moreover, we attribute this enhancement to increased levels of active GroEL, the chaperone, which, in turn, is shown for the first time to be posttranscriptionally modulated by AI-2. Such QS-mediated posttranscriptional modulation of protein levels in *E. coli* has never been reported.

MATERIALS AND METHODS

Bacterial strains and plasmid construction. The strains and plasmids used in this study are listed in Table 1. Chloramphenicol acetyltransferase (CAT) (3) and organophosphorus hydrolase (OPH) (50) were expressed using pTrcHisB (Invitrogen). In *luxS* coexpression experiments, plasmid pBO was constructed by digestion of the *opd* gene encoding organophosphorus hydrolase with NcoI and HindIII from pTO (39) and insertion into pBADHisA (Invitrogen). The *luxS* gene, after amplification by PCR from genomic DNA of strain W3110 using primers LuxSF and LuxSR (Table 2), containing EcoRI restriction sequences, was inserted into pKK223-3 (Amersham Pharmacia), yielding pKKluxS. Plasmid pBOL was constructed by PCR amplification of the *tac* promoter-*luxS* fusion from pKKluxS using primers pkk223LuxSF and pkk223LuxSR (Table 2), followed by ligation into NdeI-digested pBO. Plasmid pBOL-LacI^q was built by PCR amplification of *lacI*^{q} encoding and overproducing the Lac repressor from the vector pTrcHisB (Invitrogen), using primers LacI^{q}F and LacI^{q}R (Table 2). The PCR product was blunt cloned into BstZ17I-digested pBOL. Two additional sets of plasmids were derived from pBO, pBOL, and pBOL-LacI^q to express two other recombinant proteins, CAT and the UV-variant green fluorescent protein (GFPuv). Plasmids pBC, pBCL, and pBCL-LacI^q, carrying the PCR-amplified *cat* gene from pTrcHisCAT (Invitrogen), used similar methods and primers FCAT and RCAT (Table 2). Likewise, pBG, pBGL, and pBGL-LacI^q were constructed to express GFPuv using pTrcHisGFPuv (6) and primers FCAT and RGFPuv (Table 2). All plasmids were transformed into TOP10 competent cells (Invitrogen) for sequencing (DNA sequencing facility, University of Maryland Biotechnology Institute) and later transformed into strain W3110 or MDAI2. The recombinant model proteins were under the control of the arabinose-inducible *araBAD* promoter, and the *luxS* gene was controlled by the isopropyl-β-D-thiogalactopyranoside (IPTG)-inducible *ptac* promoter. *In vitro*-synthesized AI-2 was made by His_6-LuxS and His_6-Pfs, which were overproduced by the host, *E. coli* BL21 (Novagen) cells bearing plasmids pTrcHis-luxS and pTrcHis-pfs individually (17). *Vibrio harveyi* strains BB170 (*luxN*::Tn*5* sensor 1^- sensor 2^+) and BB152 (*luxL*::Tn*5* autoinducer-1^- autoinducer-2^+) (40) were used for AI-2

TABLE 2. Oligonucleotide primers used in this study

Name	Sequence	Relevant description
LuxSF	CCTTGAATTCAGGATGCCGTTGTTAGATAGC	Upstream primer for cloning *luxS* from W3110
LuxSR	AACTGAATTCCGGCTAGATGTGCAGTT	Downstream primer for cloning *luxS* from W3110
RTLuxSF	GATGCCGTTGTTAGATAGCTTCAC	Upstream primer for *luxS* RT-PCR
RTLuxSR	CTAGATGTGCAGTTCCTGCAAC	Upstream primer for *luxS* RT-PCR
pkk223LuxSF	ACGCATATGTCCTACTCAGGAGAGCGTTCA	Downstream primer for cloning *tac* promoter-*luxS* fusion from pKKluxS
pkk223LuxSR	AGCCATATGTCGCTCAAGGCGCACTCCCG	Downstream primer for cloning *tac* promoter-*luxS* fusion from pKKluxS
LacIqF	GGAGCTGCATGTGTCAGAGGTT	Upstream primer for cloning $lacI^q$ from pTrcHisB
LacIqR	CAAAAAACATTATCCAGAACGGGAG	Downstream primer for cloning $lacI^q$ from pTrcHisB
FCAT	TAAAAGACATGTGGGGTTCTCATCATCATC	Upstream primer for cloning *cat* and the GFPuv gene from pTrcHisCAT and pTrcHisGFPuv, respectively
RCAT2	TTAATGTTTAGCGGCCGCTTAAAAAAATTACGC	Downstream primer for cloning *cat* from pTrcHisCAT
RGFPuv	TTAATGTTTAGCGGCCGCCAGCTTTCATTATTT	Downstream primer for cloning the GFPuv gene from pTrcHisGFPuv
RTgroELF	GGCAGCTAAAGACGTAAAATTCGG	Upstream primer for *groEL* RT-PCR
RTgroELR	CATGCATTCGGTGGTGATCATC	Downstream primer for *groEL* RT-PCR
RTdnaKF	GGGTAAAATAATTGGTATCGACCTGGG	Upstream primer for *dnaK* RT-PCR
RTdnaKR	GTCTTTGACTTCTTCAAATTCAGCGTC	Downstream primer for *groEL* RT-PCR
16S-2F	AGCGCAACCCTTATCCTTTGTTGG	Upstream primer for 16S rRNA RT-PCR internal control
16S-2R	TCGCGAGGTCGCTTCTCTTTGTAT	Downstream primer for 16S rRNA RT-PCR internal control

activity assays (kindly provided by B. Bassler). Transformations, cloning procedures, and DNA isolation were performed using standard protocols (36).

Growth media. Luria-Bertani (LB) medium contained 5 g liter^{-1} yeast extract (Sigma), 10 g liter^{-1} Bacto tryptone (Difco), and 10 g liter^{-1} NaCl. *E. coli* defined growth medium was prepared according to the protocol of Riesenberg et al. (33) and supplemented with 0.8% glucose (Sigma). Autoinducer bioassay (AB) medium was made according to the protocol of Greenberg et al. (19).

Culture conditions. Primary *E. coli* inoculums, consisting of LB medium, glucose (0.8%), ampicillin (100 μg ml^{-1}; Sigma), and *E. coli* frozen stock, were grown for 4 h at 37°C with 250 rpm shaking, and then 1% (vol/vol) was inoculated into overnight cultures in defined medium (~16 h at 30°C and 250 rpm) (9). To initiate experimental cell growths, overnight cultures were inoculated into 40 ml of defined medium, and volumes were adjusted to achieve similar initial cell densities (optical density at 600 nm [OD_{600}] = 0.10). For conditioning experiments (Fig. 1), mid-log phase (OD_{600} ~ 0.25) cells were spun down gently (2,500 × *g* for 5 min at 4°C) and resuspended in either fresh defined medium, defined medium plus 10% (vol/vol) conditioned medium (CM), or defined medium plus 50% (vol/vol) CM. For coexpression experiments, arabinose (Sigma) or arabinose and IPTG (Sigma) were added to mid-log phase cultures (OD_{600} ~ 0.40).

Preparation of cell-free culture fluids and CM. Cell-free culture fluids were prepared by centrifugation of 1-ml *E. coli* whole-broth samples for 10 min (10,000 × *g* at 4°C). Cleared supernatants were passed through 0.22-μm sterile Millex filters (Millipore) and stored at −20°C. *V. harveyi* strain BB152 cell-free culture fluids were prepared likewise to obtain positive-control samples as reported previously. CM was prepared by growing *E. coli* strain W3110 or MDAI2 in LB plus 50 mM glucose or defined medium plus 50 mM glucose to an OD_{600} of 3.0 (~6 to 8 h), followed by centrifugation (10 min at 10,000 × *g* and 4°C) and filtering of cleared supernatants by vacuum-driven filter (Corning). Details of the preparation of cell-free culture fluids for AI-2 activity assays and for conditioning experiments were also described previously (9, 47).

Analytical measurements of AI-2 activity. The AI-2 activity assay was based on the reports of Surette and Bassler and Surette et al. (40, 41). Luminescence was measured hourly as a function of *V. harveyi* cell density by quantitating light production with a luminometer (EG&G Berthold). Data, reported as fold activation, were obtained by dividing the light produced by the reporter cells after the addition of *E. coli* cell-free culture fluids by the light output from the reporter cells when growth medium alone was added.

Western blot and protein activity assays. Culture volumes equivalent to 2 ml at an OD_{600} of 1.0 were withdrawn from experiments and centrifuged at 10,000 × *g* for 10 min. The cell pellets were resuspended and lysed in 300 μl BugBuster protein extraction reagent (Novagen) at room temperature for 30 min and then centrifuged again at 10,000 × *g* for 10 min to separate soluble and insoluble cell extracts. We found this lysis method to be complete, systematic, and reproducible. The protein concentration of soluble cell extracts was determined by using a protein assay kit (Bio-Rad). Insoluble cell debris was resuspended with 0.1 ml resuspension buffer (0.06 M Tris-HCl [pH 6.8]). The soluble cell extracts or insoluble debris were mixed 1:1 (vol/vol) with sodium dodecyl sulfate (SDS) sample buffer (12.5% 0.5 M Tris-HCl [pH 6.8], 10% glycerol, 2% SDS, 5% β-mercaptoethanol, 0.0025% bromophenol blue), heated at 100°C for 5 min, and centrifuged for 1 min. Samples with identical protein content were loaded onto 12.5% SDS–polyacrylamide gels for electrophoresis and blotted onto nitrocellulose membranes (Bio-Rad) using a Mini Trans-Blot cell (Bio-Rad) and Bjerrum and Schafer-Nielsen transfer buffer (48 mM Tris, 29 mM glycine, 20% methanol) for 30 min at 20 V. Monoclonal antipolyhistidine (Sigma), polyclonal anti-OPH (kindly provided by J. Grimsley), monoclonal anti-GroEL, and monoclonal anti-DnaK (Stressgen) were diluted 1:4,000 in antibody buffer (0.5% Tween 20 [vol/vol], Tris-buffered saline with 1% [wt/vol] nonfat dry milk) to probe recombinant proteins. The membranes were then transferred to a 1:4,000-diluted goat anti-mouse or goat anti-rabbit antibody conjugated with alkaline phosphatase (Sigma). Membranes were developed with 1:50-diluted Nitro Blue tetrazolium–5-bromo-4-chloro-indolyl phosphate (NBT-BCIP) solution (Roche Molecular Chemicals). Lastly, the membranes were scanned and the images were analyzed using ImageJ software (http://rsb.info.nih.gov/ij/). The activities of soluble CAT within crude cell extracts were measured according to the method of Rodriguez and Tait (34), OPH activities were measured according to the method of Wu et al. (50), and the GFP activities of 1-ml whole-cell samples were measured using a Perkin-Elmer LS-3B fluorescence spectrometer at excitation and emission wavelengths of 395 and 509 nm, respectively. Finally, specific CAT and OPH activities were reported as activity divided by total protein concentration (34, 50).

RT-PCR. To determine the relative transcription levels of the genes of interest (i.e., *luxS*, *groEL*, and *dnaK*), cell pellets were lysed and RNA extracted using an RNAqueous kit (Ambion) according to the manufacturer's instructions. The total RNA concentration was determined by measuring the absorbance of a diluted sample at 260 nm using a UV spectrophotometer (Beckman). To synthesize cDNA, 300 ng total RNA was subjected to reverse transcription (RT) using gene-specific primers. The cDNA was used as the template in PCR with gene-specific primers. The primer sets used for RT-PCR are listed in Table 2. PCR products were run on a 1% agarose gel to compare band intensities using ImageJ software (http://rsb.info.nih.gov/ij/). All data were normalized to the levels of the internal control, endogenous 16S rRNA.

Synthesis and fractionation of *in vitro* AI-2. His_6-Pfs and His_6-LuxS were overexpressed (17, 37) under 1 mM IPTG induction of BL21(pTrcHis-pfs) and BL21(pTrcHis-luxS) as cell densities were grown to OD_{600} values of ~0.4 to 0.6 at 37°C. The cells were harvested 4 h postinduction (h.p.i.) by centrifugation at 14,000 × *g* for 20 min at 4°C. After lysis using BugBuster solution (Novagen) at room temperature for 40 min, the soluble cell extracts were mixed with Co^{2+} affinity resin (BD Talon; BD Biosciences), and the bound His_6-Pfs and His_6-LuxS were washed three times using phosphate buffer (pH 7.4) (Sigma) to remove nonspecifically bound proteins. The purified enzymes were eluted (125 mM

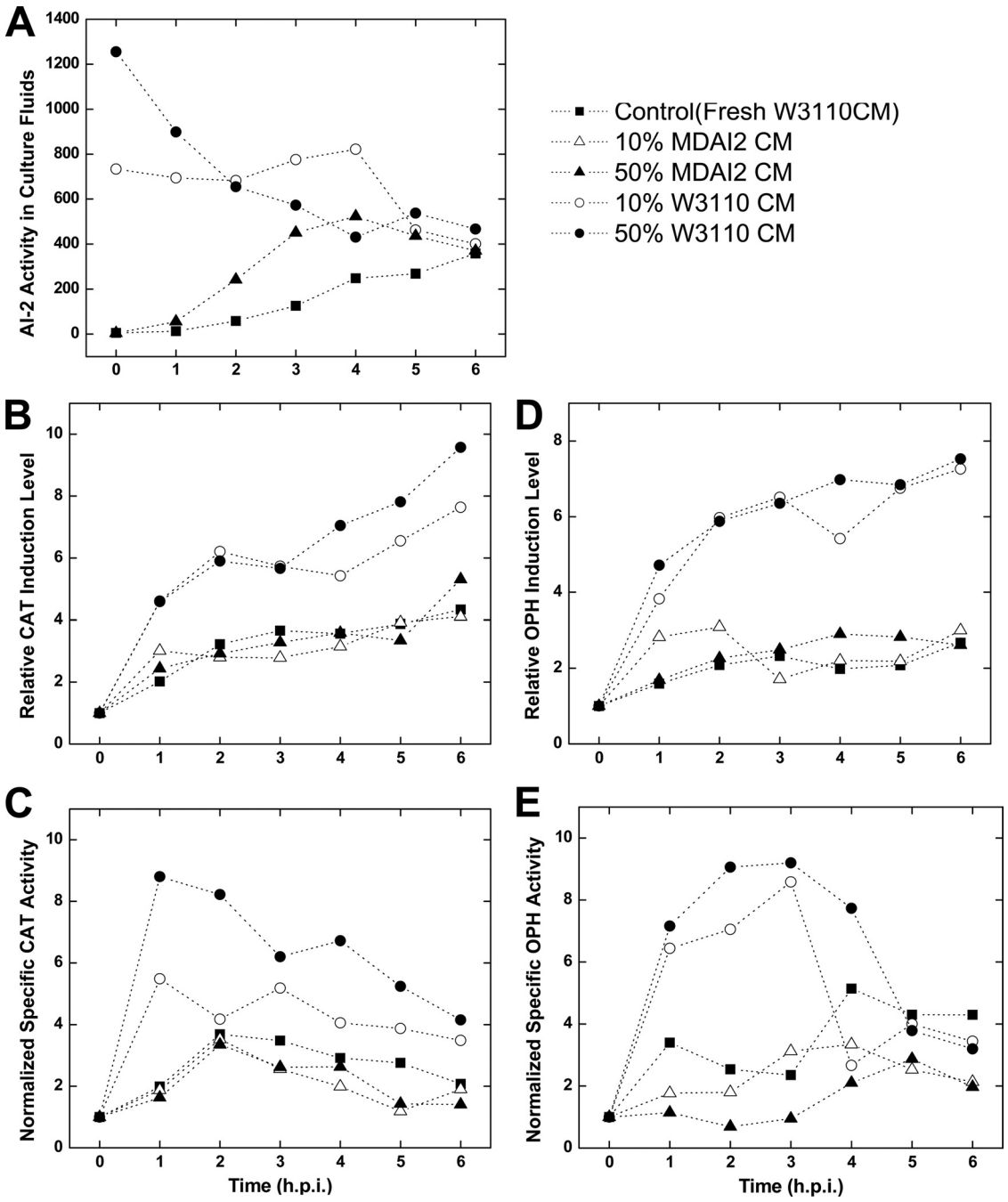

FIG. 1. Supplementation with AI-2-containing conditioned medium enhances recombinant protein production. The AI-2 level in W3110/pTrcHis-CAT or -OPH cell cultures was modulated by resuspending cells in CM containing AI-2 activity (circles; generated from wild-type strain W3110) or lacking AI-2 activity (triangles; generated from *luxS*-deficient MDAI2 cells). Recombinant protein expression was induced at $t = 0$ h (1 mM IPTG). (A) AI-2 activity in W3110/pTrcHis-CAT culture fluids. (B and C) Relative CAT induction level (normalized by total protein concentration) (B) and normalized specific CAT activity (C). These results demonstrate that exogenously added AI-2 enhances CAT production. (D and E) Similar results were found for W3110/pTrcHis-OPH. Induction levels (normalized by total protein concentration) and normalized specific activities are reported as the Western blot band intensity and specific activity, respectively, of each sample relative to the preinduction ($t = 0$ h) value. The reported blot intensities and activity levels are the average results of duplicate experiments and agree to within 15%.

imidazole in phosphate buffer, pH 7.4) and used to synthesize AI-2 from 1 mM *S*-adenosylhomocysteine (SAH) in 50 mM Tris-HCl (pH 7.8) at 37°C for 4 h (17). The enzymatic reaction product was extracted twice with chloroform and recovered from the aqueous phase. To remove unreacted SAH substrate and the by-products adenine and homocysteine, the *in vitro* AI-2 reaction product was fractionated by high-performance liquid chromatography (HPLC) with a preparative silica reverse-phase column (25 by 10 cm), using 90% water–10% acetonitrile eluent at a flow rate of 3 ml/min (Dynamax SD-200 pumps; Varian, Inc., Walnut Creek, CA). Absorbance at 210 nm and 260 nm was recorded using a UV-D II dual-wavelength UV-visible light detector (see Fig. S2 in the supplemental material). After fractionation, acetonitrile was evaporated from each aliquot for 1.5 h by using a CentriVap concentrator (Labconco) and analyzed for

AI-2. Fractionated *in vitro* AI-2 was further confirmed by mass spectrometry using JEOL AccuTOF-CS ESI-TOF mass spectrometers (dual electrospray ionization; mass ranges from 100 to 1,000 *m/z* were monitored) (see Fig. S3 in the supplemental material) and AI-2 activity bioassay.

RESULTS

"AI-2-conditioned cultures" exhibit increased chloramphenicol acetyltransferase and organophosphorus hydrolase. In earlier studies, we observed significant drops in AI-2 levels after the induction of recombinant proteins (9). Here, a simple study was performed in which conditioned medium (CM) with or without AI-2 was added to cultures at the same time as the inducer (IPTG). W3110/pTrcHis-CAT and -OPH cells were cultured to mid-log phase and resuspended in various concentrations of conditioned media (10% and 50%) from AI-2-producing (+AI-2) or *luxS* mutant (−AI-2) cells and then immediately induced with 1 mM IPTG. In CAT-producing cultures, AI-2 was initially highest under the 10% and 50% CM (+AI-2) conditions and progressively dropped to the control levels thereafter (Fig. 1A). Similar results were obtained for *E. coli* cultures producing OPH (not included here). W3110 produces AI-2 via the normal metabolic pathways, and MDAI2 is an isogenic *luxS* mutant. Our results suggest behavior due to an imposed large differential in AI-2 activity with, presumably, few other differences in the CM (10).

Remarkably, the expression levels of CAT (25 kDa) and OPH (36 kDa) both increased 2- to 4-fold relative to the levels in control cells identically resuspended in CM from MDAI2 cells (−AI-2) (Fig. 1B and D). In both cases, the specific activities increased concomitantly, with activities in +AI-2 CM cultures reaching 4-fold higher than in controls (Fig. 1C and E). The specific activities reported are the activities of the enzymes normalized by the mass of each protein expressed, obtained via Western blot. The cell growth rates were unaffected by the conditioned media during the times indicated. We also note that the enhancements observed were typically greatest during the periods when the AI-2 levels were most disparate (first 3 h).

Construction of controllable LuxS coexpression system. Because CM is poorly defined, we designed a system to link enhanced yield to AI-2. We constructed LuxS coexpression vectors for *in vivo* generation of AI-2, as well as recombinant proteins, wherein LuxS and the product proteins were independently controlled under different controllable promoters. MDAI2, a *luxS* null mutant host, was used as the background host to enable a full range of AI-2 "tuning" (from near zero [mutant] to high levels [LuxS overexpression]). In addition, the MDAI2 background eliminates interplay between genomic *luxS* and genome-synthesized AI-2 and that produced via the plasmids. Organophosphorus hydrolase (OPH) was selected as a model product because its expression in *E. coli* has proved difficult (50). For coexpression, an IPTG-inducible *luxS* sequence was inserted into pBO to make pBOL, which produces OPH under the control of the arabinose-inducible *araBAD* promoter (Fig. 2A). Further, to minimize background *luxS* transcription, *lacI*^{q} was inserted into pBOL, yielding pBOL-LacI^q (Fig. 2A). These vectors enable independent control of *luxS* and *opd*.

To determine whether *luxS* expression could modulate the AI-2 levels measured in extracellular medium, MDAI2(pBOL-LacI^q) cells were grown to mid-log phase ($OD_{600} \approx 0.4$) in defined minimal medium supplemented with 0.8% glucose which, in turn, ensures high AI-2 activity (40, 47, 51). IPTG was added at various levels (0 to 1 mM) after 5 h of growth; the AI-2 levels in the extracellular medium spanned a 150-fold range after an additional 4 h. The immediate AI-2 activity differences (<1 h) were substantially smaller, but a 25-fold difference was ultimately observed between the 0 and 1 mM IPTG conditions. These results, not surprisingly, confirm that LuxS expression encoded by these *luxS* coexpression vectors

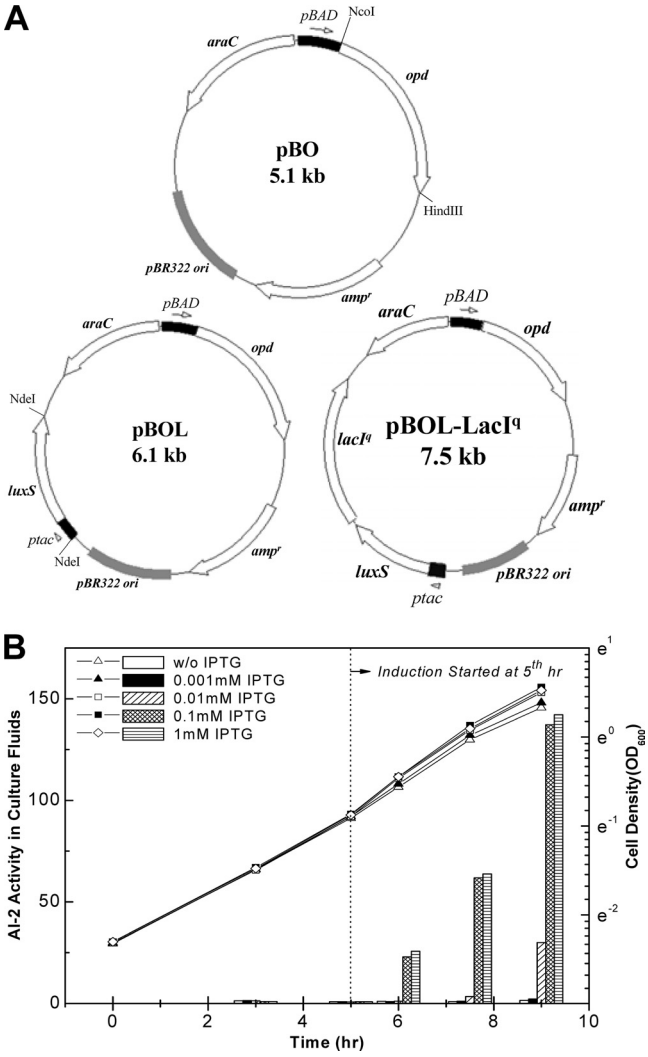

FIG. 2. LuxS and recombinant protein coexpression vectors. (A) pBO expresses *opd* under the control of the arabinose-inducible promoter *araBAD*. An expression cassette of the IPTG-inducible promoter *ptac* and the *luxS* gene was inserted into pBO, yielding pBOL. To more effectively regulate *luxS* expression, LacI^q was inserted into pBOL, yielding pBOL-LacI^q. (B) Modulation of AI-2 via varied *luxS* expression was carried out by the addition of different concentrations of IPTG to MDAI2 (pBOL-LacI^q) cultures. At different time points during cell growth, aliquots were collected for measurement of cell density (lines) and AI-2 activity (bars). The AI-2 values shown here are representative of three independent experiments. The replicate assays agreed within 15%. w/o, without.

within the *luxS* mutant can modulate the AI-2 level in the extracellular medium.

Coexpression of LuxS improves recombinant OPH protein production in strain MDAI2. Wild-type *E. coli* W3110 and the *luxS* isogenic knockout MDAI2 were transformed with plasmids pBO, pBOL, and pBOL-LacI^q and grown to mid-log phase ($OD_{600} \approx 0.4$) in defined minimal medium containing 0.8% glucose. Arabinose (0.2%) was added to each culture to induce *opd*. Additionally, the cultures containing pBOL-LacI^q were grown with and without 0.01 mM IPTG, the inducer of *luxS*. We found that 0.01 mM IPTG was sufficient to generate but not rapidly accumulate AI-2 in the extracellular fluids (Fig. 3A, similar to Fig. 2). Figure 3B depicts the levels of *luxS* mRNA, which were highest for the pBOL vector in the *luxS* mutant, lowest for the pBO vector in the *luxS* mutant, very low for the uninduced *lacI*^{q}-repressed vector, and somewhat higher for the same vector minimally induced (0.01 mM IPTG). The results obtained by image analysis suggest a linear correlation between *luxS* mRNA and AI-2 levels within MDAI2, with the highest level of AI-2 corresponding to the highest level of mRNA (pBOL). In wild-type cells, we found more extracellular AI-2 per *luxS* mRNA and have no explanation other than perhaps an alternative metabolic effect associated with the *luxS* mutation (29). The growth rates of MDAI2(pBOL-LacI^q) with and without *luxS* induction were both slightly lower than the growth rates of MDAI2(pBO) and MDAI2(pBOL) (Fig. 3A).

The OPH yield in the MDAI2(pBO) culture was unchanged relative to that of the W3110(pBO) culture. Restoring *luxS* under *ptac* promoter control on pBOL resulted in slightly less AI-2 than for W3110 and a relatively unchanged level of OPH. Remarkably, for MDAI2(pBOL-LacI^q) under both conditions, a 3- to 4-fold increase in specific OPH activity was observed (Fig. 3C). In the experiment whose results are shown in Fig. 3D, we found an appreciable increase (~1.5-fold) in OPH in the soluble fraction of cell extracts. The level of OPH found in the insoluble fractions was similar among all cultures (Fig. 3E). The nearly 1.5-fold increase in soluble OPH at 4 h.p.i., however, was insufficient to account for the increased activity per mg protein (4-fold) (Fig. 3C). Thus, the OPH was of higher specific activity (quality) and higher yield (quantity). The results depicted in Fig. 3 demonstrate that within MDAI2 cells, *luxS* expression led to increased AI-2 accumulation and altered OPH yield and activity. Presumably there was a relationship between *luxS* expression and the protein synthesis machinery. In order to test whether the enhanced yield was OPH specific, we repeated these experiments with additional recombinant proteins (9).

CAT and GFPuv coexpressed with LuxS. We replaced the *opd* gene in the plasmids noted above (pBO, pBOL, and pBOL-LacI^q) with *cat* or the GFPuv gene, respectively, for the overexpression of CAT and GFPuv. Again, W3110 and MDAI2 were transformed with the expression plasmids, and LuxS coexpression experiments were executed under the same conditions as described above. In all cases, coexpression of LuxS increased the specific activities of the recombinant model proteins, CAT (~1.5-fold) and GFPuv (~4- to 6-fold) (Fig. 4). The protein expression levels were also investigated via Western blot analysis. Both CAT and GFPuv were found to increase in both soluble and insoluble fractions (not shown). These data support the conclusion that enhanced yield via LuxS coexpression is protein independent.

The chaperone protein GroEL is affected by *luxS* coexpression. Protein chaperones, including GroEL, play key roles in the assembly and folding of heterologous proteins expressed in *E. coli* (18, 42). Coexpression of GroEL is often used to improve folding and enhance yield (16). It is also recognized that the abundance of heat shock proteins (HSPs, including chaperones and proteases) is influenced by heterologous protein overexpression and, in turn, can affect the protein yield (4, 14, 21, 23, 32, 42). We have previously demonstrated that avoiding (32) or intentionally downregulating (39) the heat shock response coincident with protein overexpression, as well as stimulation of HSPs prior to induction (14), can facilitate increased yield and activity of CAT (14) and OPH (39). To ascertain whether *luxS* coexpression leads to increased yield through the pleiotropic regulation of HSPs, we measured the levels of two important heat shock proteins, GroEL and DnaK, as well as the transcription of these and several other proteins in the presence and absence of varied LuxS expression (48).

The amounts of GroEL and DnaK in MDAI2 cultures induced with arabinose to synthesize OPH were examined by Western blotting at both 1 and 4 h.p.i. (Fig. 5). In all cases where *luxS* was introduced in *trans*, the GroEL levels in the soluble fractions were higher (up to ~3- to 4-fold) than in controls [W3110(pBO) and MDAI2(pBO)] (Fig. 5A). The GroEL levels in the insoluble fractions of all cultures were similar in all cases (Fig. 5B). The DnaK levels in the soluble fractions were typically unchanged, although there was a 60% increase in the cases where LuxS was regulated by LacI^q (Fig. 5C). There was no detectable DnaK in any of the insoluble fractions (not shown). Importantly, in the cases where soluble GroEL increased the most (MDAI2 with *lacI*^{q}, with or without IPTG), we found the highest and most active levels of OPH (Fig. 3C and D).

While the overexpression of nonnative proteins has previously been shown to increase the levels of GroEL and DnaK in *E. coli* (23, 39), we attempted to explore whether LuxS and/or AI-2 had an independent effect on these important chaperones, irrespective of the recombinant product. Hence, MDAI2(pBOL-LacI^q) cultures were supplemented with different levels of IPTG to vary LuxS expression, and the two chaperones were examined by Western blotting (Fig. 5D to F). Results for AI-2 in these experiments are also shown in Fig. 2 and show altered levels of *luxS* induction with no background *opd* expression (as confirmed by activity measurements; data not shown). Interestingly, GroEL was notably upregulated in the soluble fractions in cultures with IPTG at or above 0.01 mM (Fig. 5D) and was moderately downregulated in the insoluble fractions of the same cultures (Fig. 5E). There were no significant differences in the levels of in DnaK found in the soluble fractions (Fig. 5F), and there was no observable DnaK in the insoluble fractions (not shown). These results demonstrate that LuxS expression in a *luxS*-deficient host can modulate the levels of GroEL in both the soluble and insoluble fraction and suggest that an appropriate LuxS expression level could be found that is coincident with an appropriate GroEL level that facilitates the folding of target proteins in *E. coli*.

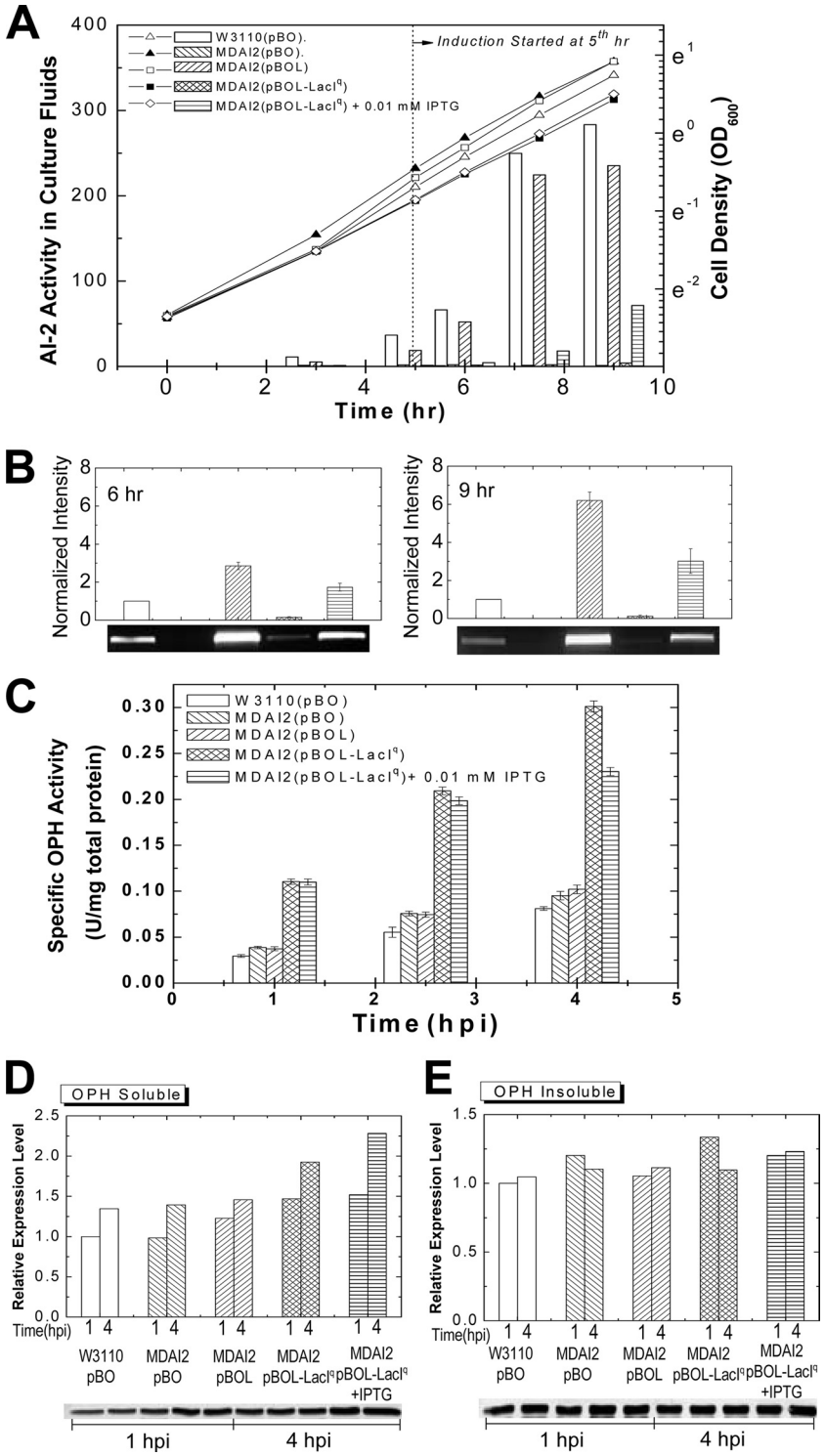

FIG. 3. OPH accumulation and activity are both enhanced significantly by modulating LuxS expression in a coexpression system. (A) OPH was expressed in *E. coli* W3110 (wild type) and MDAI2 (*luxS* deficient) by 0.2% arabinose induction and altered AI-2 signaling. That is, MDAI2(pBOL-LacI^q) cultures with and without 0.01 mM IPTG were compared with W3110(pBO), MDAI2(pBO), and MDAI2(pBOL) cultures when identical levels of arabinose (0.2%) were added. Throughout, the cell densities (lines) and AI-2 activities (bars) were observed. (B) Transcriptional analysis of *luxS* for OPH expression in the coexpression system. The RNA was extracted from 1-h.p.i. and 3-h.p.i. samples, and an agarose gel was run to show *luxS* mRNA levels from RT-PCR using *luxS* gene-specific primers. (C) After induction, samples were collected and lysed. The OPH activity in each sample was measured and divided by the total protein concentration to derive the specific OPH activity. The data shown here are representative of two independent experiments. The errors shown are standard errors from triplicate OPH activity and total-protein assays. (D and E) OPH accumulation in the soluble (D) and insoluble (E) fractions of cell extracts was examined 1 h.p.i. and 4 h.p.i. by Western blotting. The results shown here are not pooled but, instead, are representative of triplicate experiments (which agreed to within 20%).

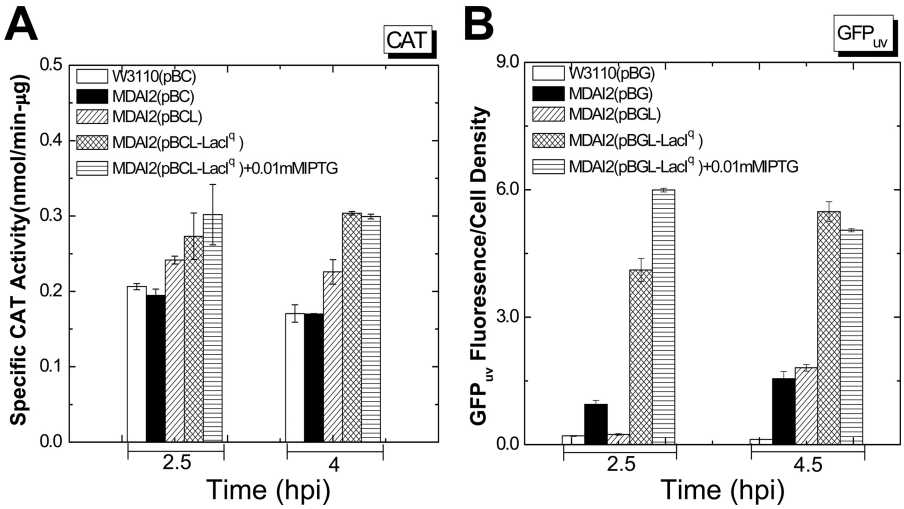

FIG. 4. Specific activities of CAT (A) and GFPuv (B) are enhanced in the LuxS coexpression system. CAT (A) and GFPuv (B) were expressed in *E. coli* W3110 and MDAI2 by 0.2% arabinose induction and at different AI-2 levels (by varied IPTG concentrations). CAT activities were divided by the total protein level of each cell extract to generate the specific CAT activities. However, in order to derive specific GFPuv activities, the fluorescence results for GFPuv were divided by the cell density (OD_{600}) directly instead of by the total protein concentration of each sample. Both the CAT and the GFPuv coexpression experiments were duplicated to confirm reproducibility; the data shown here are representative, and the standard errors from triplicate assays are shown.

Does AI-2 communicate with GroEL? In these experiments, LuxS expression was altered and the yields of several recombinant proteins were increased. Moreover, we observed that the chaperone GroEL was upregulated, both in response to the addition of arabinose and IPTG for the expression of recombinant protein products and LuxS and in response to IPTG for the expression of LuxS alone. To investigate whether the expression of LuxS led to increased GroEL (as a stress response) or whether AI-2 signaling played a role, we added *in vitro*-synthesized AI-2 (Fig. 6A) (17, 38) or mock-synthesized-AI-2 synthesis buffer (negative control) to MDAI2 cells. The AI-2 levels in treated MDAI2 cultures decreased steadily, and growth rates were unaffected (data not shown). The two chaperones, GroEL and DnaK, were observed by Western blot analysis (Fig. 6B to D shows the results at 1 h.p.i.). GroEL increased ~1.5- to 2-fold in the soluble fractions for the first hour when AI-2 was added (20× to 100× dilutions). Moreover, GroEL appeared to increase with AI-2 in a concentration-dependent manner. A slight but statistically insignificant decrease in the level of GroEL in the insoluble fraction was also observed (Fig. 6C). There was no observable trend in soluble DnaK (Fig. 6D), and no insoluble DnaK was detected under any of the conditions (data not shown). Additionally, the results at 2 h.p.i. showed no conclusive changes in GroEL or DnaK levels in response to AI-2. In the experiments whose results are shown in Fig. 6E and F, the corresponding levels of mRNA were measured, and no changes due to the addition of AI-2 were found. We have previously performed genome-spanning DNA microarray analyses on W3110 and MDAI2 (*luxS*-deficient) cells grown with and without glucose, as well as LsrK mutants exhibiting no phosphorylated AI-2, and found no significant differences in the transcription of GroEL or DnaK. Conversely, Kendall and coworkers (24) found increased transcription of GroEL in a *luxS* mutant relative to that in its isogenic parent but no further increase in *groEL* mRNA upon the addition of DPD.

In summary, our results shown in Fig. 6 demonstrate an increased level of soluble GroEL in a *luxS* mutant supplemented with *in vitro*-synthesized AI-2. Our results shown in Fig. 6E and F, confirming the results of Kendall et al. (24), demonstrate a negligible increase in *groEL* transcription in *luxS* mutants supplemented with AI-2. Because the QS signal molecule AI-2 affects the level of GroEL in the soluble fraction of *E. coli*, we suggest that LuxS expression in *luxS* mutants can alter the levels of chaperone GroEL in soluble fractions through AI-2-mediated signaling.

DISCUSSION

Studies of AI-2-mediated QS suggest that quorum signaling may communicate the prevailing metabolic condition (8, 9) and that a tweaked signaling process may potentially enable improved recombinant protein production. By the results shown in Fig. 1, we demonstrate for the first time that the addition of exogenous AI-2-containing CM enhances CAT and OPH production both in quantity (protein yield) and quality (protein activities). Recognizing the possibility that many metabolites may have altered concentrations in CM from *luxS*-deficient versus *luxS*-positive strains (7, 25), we developed a controlled study to investigate *luxS*/AI-2 QS during recombinant protein overexpression. Furthermore, because commercial bioprocesses are unlikely to allow the addition of uncharacterized CM to bioreactors, we developed the "tunable" dual-controlled expression vector in which AI-2 synthesis and product synthesis are uncoupled and independently exogenously regulated.

Both the expression level and activity of the recombinant product were increased when *luxS*-deficient (MDAI2) cells

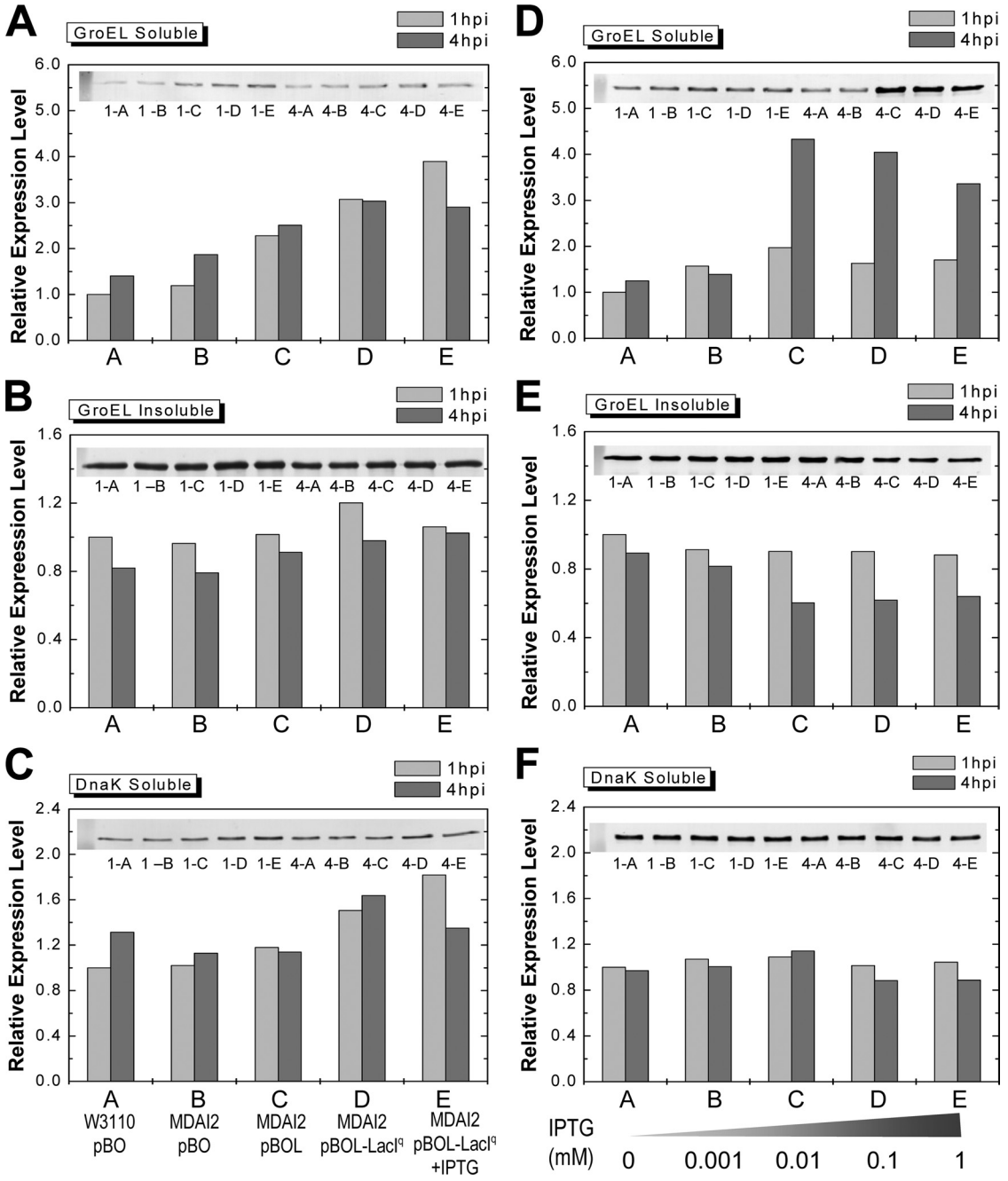

FIG. 5. The expression levels of chaperone protein GroEL in soluble cell extracts were significantly higher than in controls in the *luxS*-modulated system. (A, B, and C) The amounts of GroEL and DnaK in cultures induced with arabinose to synthesize OPH were examined at both 1 and 4 h.p.i. by Western blotting. MDAI2(pBOL-LacI^q) cultures with and without 0.01 mM IPTG were compared with W3110(pBO), MDAI2(pBO), and MDAI2(pBOL) cultures when identical levels of arabinose (0.2%) were added. The lanes are labeled with 1 or 4 for the time (h) postinduction and A, B, C, D, or E for the strains and plasmids, indicated below the panels. (D, E, and F) MDAI2(pBOL-LacI^q) cultures were supplemented with different concentrations of IPTG to vary LuxS expression in the absence of recombinant protein synthesis. GroEL and DnaK were examined by Western blotting. In this case, A, B, C, D, and E correspond to different concentrations of IPTG, shown below the panels.

were complemented with *luxS* under *lacI*^{q} control. The *luxS* expression levels in these cultures were in the middle of our tested range [from none in the MDAI2(pBO) cells to maximum levels in the MDAI2(pBOL) cells]. In Fig. S1 in the supplemental material, we demonstrate that increased yield was not due to LacI^q; rather, our results suggest that an intermediate level of *luxS* expression (obtained by *luxS* expression under LacI^q control) was optimal. It is interesting to note that this "optimal" level actually led to intermediate levels of AI-2, as well (compare Fig. 2 to Fig. 3). Hence, the main contributor to the benefits in yield and activity was the manipulation of *luxS*. We also demonstrated that for all cases of dramatically

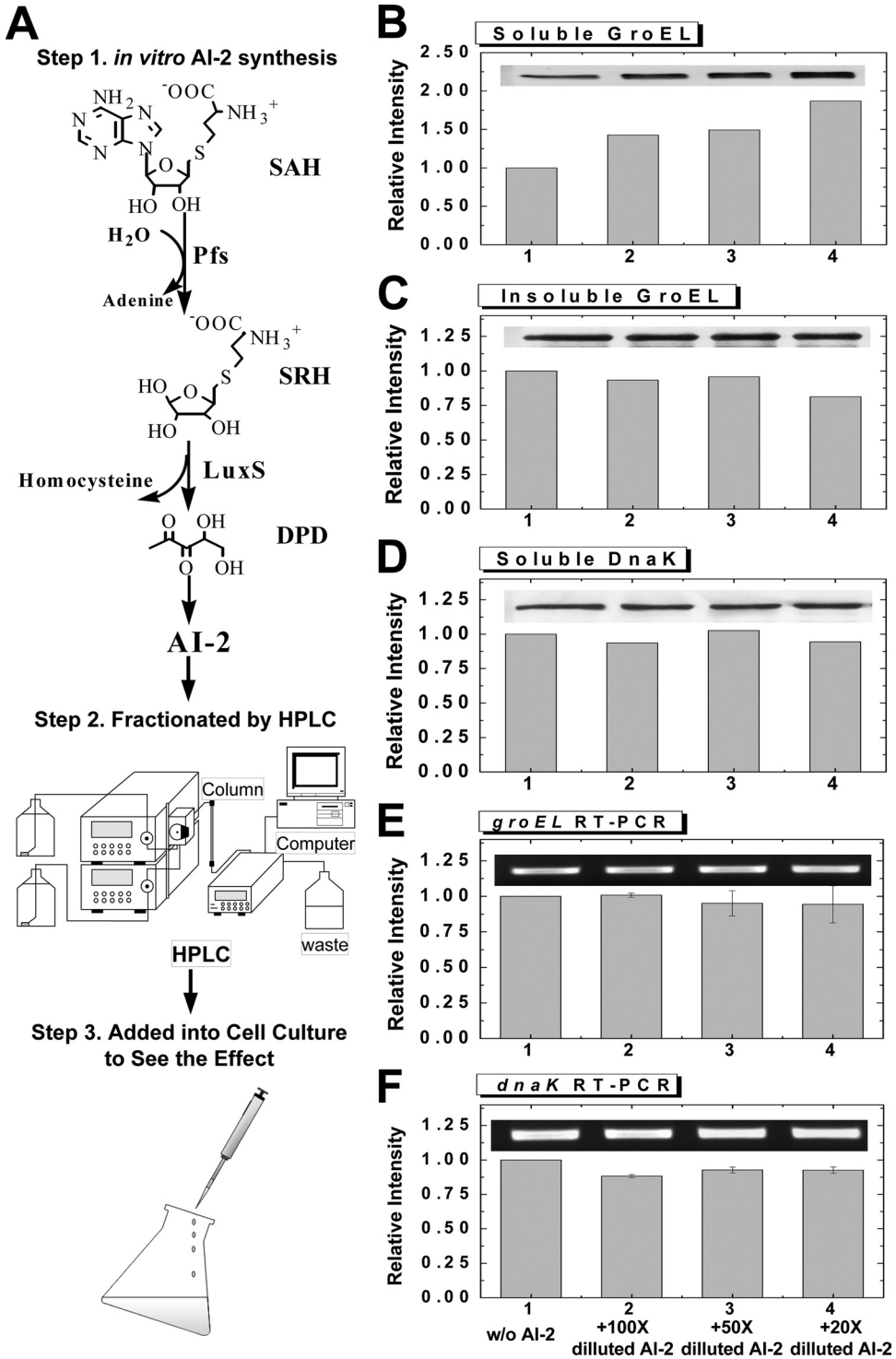

FIG. 6. *In vitro*-synthesized AI-2 increases soluble GroEL level. (A) The scheme depicts the synthesis and fractionation of AI-2 and its addition to cell cultures of MDAI2 (no plasmid). First, AI-2 was synthesized *in vitro* from substrate SAH. Second, any unreacted SAH and by-products homocysteine and adenine were removed by HPLC. After mobile-phase solvent removal via vacuum pump, the fractionated AI-2 was added to MDAI2 cell cultures. (B to D) Samples were taken at 1 h.p.i. Chaperones GroEL (soluble [B] and insoluble [C] fractions) and DnaK (soluble fraction [D]) were analyzed by Western blotting. The results shown here are representative of duplicate experiments and triplicate assays. (E and F) Transcriptional analysis of *groEL* (E) and *dnaK* (F) indicating no change due to the addition of AI-2. Error bars show standard error. Western blotting and RT-PCR were performed within the linear ranges of the assays.

improved recombinant protein production, the GroEL level was increased in the soluble fractions (Fig. 3 and 5, respectively).

Upregulation of HSPs, including GroEL and DnaK, is commonly observed to accompany recombinant protein overexpression, due to an upregulated heat shock response (4, 8, 21, 23, 32, 42). That is, increases in both *groEL* and *dnaK* transcription (8) and GroEL and DnaK protein levels (4, 21, 23, 32) are typically observed. The influence of *luxS* coexpression in the $LacI^q$ experiments (Fig. 5A and C, bars D and E) points to the coordinate change in GroEL and DnaK when there is an abundance of recombinant protein overexpression. This is likely coincident with an upregulated stress response. For this reason, we undertook the systematic study of GroEL and DnaK in the absence of protein overexpression (Fig. 5D to F). In these experiments, there was a decoupling of GroEL from DnaK, suggesting that the differences observed were due to *luxS* abundance and, perhaps, AI-2 signaling (the *luxS*-related influence is likely obscured in the overexpression experiments). This conclusion is strengthened by the apparent exchange between soluble and insoluble GroEL in Fig. 5D and E. Indeed, throughout the study, DnaK levels exhibited no systematic trend.

Finally, *dnaK* and *groEL* transcription in W3110 and MDAI2 are unaltered by *luxS* mutation (48) and AI-2 signaling, as demonstrated by our analysis of LsrRK mutations (28) and microarray data for the addition of exogenous AI-2 (24). Their transcription rates are seemingly uncorrelated with QS. Hence, the apparent decoupling of (i) the GroEL level in the soluble fraction from its transcription level and (ii) the levels of GroEL protein and DnaK suggested that the enhanced levels of GroEL were due to other mechanisms than the classic heat shock-like response (15, 18, 23, 38). Since *groEL* transcription is apparently unaffected by AI-2, we suggest that the apparent linkage between the GroEL level and *luxS* coexpression is at the posttranscriptional level. We are aware of only one report in which an AI-2-mediated process was found to affect the level of a protein in a manner other than transcriptional regulation. In that report, the AI-2 phosphorelay system of *V. harveyi* is shown to affect endogenous *lux* enzyme activity by modulating translation through the recruitment of small RNAs (sRNA) and the RNA chaperone Hfq (26). Interestingly, Guisbert et al. (20) demonstrated Hfq functions in *E. coli* and the Hfq-mediated decoupling of GroEL and DnaK translation. In the same report, they showed reduced GroEL translation in an Hfq mutant, suggesting that the GroEL-mediated negative-feedback control of σ^{32} was preserved, as well as long-term adaptation. They also reported that DnaK translation was suppressed by Hfq. Our results, with unchanged DnaK and upregulated GroEL, are seemingly contradictory, assuming that Hfq acts in concert with QS-regulated sRNA in a manner exactly analogous to that in *V. harveyi*. We have previously shown that AI-2 signaling influences sRNA (28), but there remains no evidence that any QS-regulated sRNA interacts with Hfq. That these components all seem to be functioning in *E. coli* does suggest that further work is warranted.

While there have been no reports of posttranscriptional regulation in *E. coli* that are attributed to QS, we found that the level of GroEL in the soluble fraction increased significantly within the first hour in experiments where purified AI-2 was added to cultures of MDAI2. Also, we found in several cases that the increase was accompanied by a decrease in the level in the insoluble fraction, again suggesting that there was no apparent linkage between AI-2 and *groEL* transcription. That DnaK has no insoluble reservoir in our experiments reinforces the notion of differential AI-2-mediated regulation. Irrespective of the exact cause (via sRNA, Hfq, or other factors), we believe this is the first demonstration that AI-2 alters the level of GroEL in the soluble fraction in *E. coli*. Moreover, it is well known that GroEL assists in the production of properly folded recombinant proteins (16, 18, 42, 43). The results of this study suggest that altered AI-2 signaling (by *luxS* coexpression) can be used to improve recombinant protein yield in *E. coli.* While there are many functions that are altered by *luxS* coexpression, we observed AI-2-mediated posttranscriptional modulation of GroEL and hypothesize that this was a contributing factor and could have been a very significant factor in the increased yield and activities observed.

ACKNOWLEDGMENTS

Partial support of this work was provided by the National Science Foundation (grant no. BES-0222687 and BES-0124401) and the U.S. Army.

REFERENCES

1. **Ahmer, B. M. M.** 2004. Cell-to-cell signalling in *Escherichia coli* and *Salmonella enterica*. Mol. Microbiol. **52:**933–945.
2. **Bassler, B. L., M. Wright, R. E. Showalter, and M. R. Silverman.** 1993. Intercellular signalling in *Vibrio harveyi*: sequence and function of genes regulating expression of luminescence. Mol. Microbiol. **9:**773–786.
3. **Bentley, W. E., R. H. Davis, and D. S. Kompala.** 1991. Dynamics of induced CAT expression in *E. coli*. Biotechnol. Bioeng. **38:**749–760.
4. **Bentley, W. E., N. Mirjalili, D. C. Andersen, R. H. Davis, and D. S. Kompala.** 1990. Plasmid-encoded protein: the principal factor in the metabolic burden associated with recombinant bacteria. Biotechnol. Bioeng. **35:**668–681.
5. **Bulter, T., et al.** 2004. Design of artificial cell-cell communication using gene and metabolic networks. Proc. Natl. Acad. Sci. U. S. A. **101:**2299–2304.
6. **Cha, H. J., C. F. Wu, J. J. Valdes, G. Rao, and W. E. Bentley.** 2000. Observations of green fluorescent protein as a fusion partner in genetically engineered *Escherichia coli*: monitoring protein expression and solubility. Biotechnol. Bioeng. **67:**565–574.
7. **DeLisa, M. P., and W. E. Bentley.** 2002. Bacterial autoinduction: looking outside the cell for new metabolic engineering targets. Microb. Cell Fact. **1:**5.
8. **DeLisa, M. P., J. J. Valdes, and W. E. Bentley.** 2001. Mapping stress-induced changes in autoinducer AI-2 production in chemostat-cultivated *Escherichia coli* K-12. J. Bacteriol. **183:**2918–2928.
9. **DeLisa, M. P., J. J. Valdes, and W. E. Bentley.** 2001. Quorum signaling via AI-2 communicates the "metabolic burden" associated with heterologous protein production in *Escherichia coli*. Biotechnol. Bioeng. **75:**439–450.
10. **DeLisa, M. P., C. F. Wu, L. Wang, J. J. Valdes, and W. E. Bentley.** 2001. DNA microarray-based identification of genes controlled by autoinducer 2-stimulated quorum sensing in *Escherichia coli*. J. Bacteriol. **183:**5239–5247.
11. **Domka, J., J. Lee, and T. K. Wood.** 2006. YliH (BssR) and YceP (BssS) regulate *Escherichia coli* K-12 biofilm formation by influencing cell signaling. Appl. Environ. Microbiol. **72:**2449–2459.
12. **Fuqua, C., and E. P. Greenberg.** 1998. Cell-to-cell communication in *Escherichia coli* and *Salmonella typhimurium*: they may be talking, but who's listening? Proc. Natl. Acad. Sci. U. S. A. **95:**6571–6572.
13. **Fuqua, C., and E. P. Greenberg.** 1998. Self perception in bacteria: quorum sensing with acylated homoserine lactones. Curr. Opin. Microbiol. **1:**183–189.
14. **Gill, R. T., M. P. DeLisa, J. J. Valdes, and W. E. Bentley.** 2001. Genomic analysis of high-cell-density recombinant *Escherichia coli* fermentation and "cell conditioning" for improved recombinant protein yield. Biotechnol. Bioeng. **72:**85–95.
15. **Gill, R. T., J. J. Valdes, W. E. Bentley, and W. E. Bentley.** 2000. Analysis of differential stress gene transcription in response to recombinant protein over-expression and high cell density fermentation in *Escherichia coli*, abstr. BIOT159. *In* Abstr. 219th ACS National Meeting, San Francisco, CA, 26 to 30 March 2000. American Chemical Society, Washington, DC.
16. **Goloubinoff, P., A. A. Gatenby, and G. H. Lorimer.** 1989. Groe heat-shock proteins promote assembly of foreign prokaryotic ribulose bisphosphate carboxylase oligomers in *Escherichia coli*. Nature **337:**44–47.

17. **González Barrios, A. F., et al.** 2006. Autoinducer 2 controls biofilm formation in *Escherichia coli* through a novel motility quorum-sensing regulator (MqsR, B3022). J. Bacteriol. **188:**305–316.
18. **Gragerov, A., et al.** 1992. Cooperation of GroEL/GroES and DnaK/DnaJ heat-shock proteins in preventing protein misfolding in *Escherichia coli*. Proc. Natl. Acad. Sci. U. S. A. **89:**10341–10344.
19. **Greenberg, E. P., J. W. Hastings, and S. Ulitzur.** 1979. Induction of luciferase synthesis in *Beneckea-Harveyi* by other marine bacteria. Arch. Microbiol. **120:**87–91.
20. **Guisbert, E., V. A. Rhodius, N. Ahuja, E. Witkin, and C. A. Gross.** 2007. Hfq modulates the σ^E-mediated envelope stress response and the σ^{32}-mediated cytoplasmic stress response in *Escherichia coli*. J. Bacteriol. **189:**1963–1973.
21. **Harcum, S. W., and W. E. Bentley.** 1993. Detection, quantification, and characterization of proteases in recombinant *Escherichia coli*. Biotechnol. Tech. **7:**441–447.
22. **Hastings, J. W., and E. P. Greenberg.** 1999. Quorum sensing: the explanation of a curious phenomenon reveals a common characteristic of bacteria. J. Bacteriol. **181:**2667–2668.
23. **Kanemori, M., H. Mori, and T. Yura.** 1994. Induction of heat shock proteins by abnormal proteins results from stabilization and not increased synthesis of σ^{32} in *Escherichia coli*. J. Bacteriol. **176:**5648–5653.
24. **Kendall, M. M., D. A. Rasko, and V. Sperandio.** 2007. Global effects of the cell-to-cell signaling molecules autoinducer-2, autoinducer-3, and epinephrine in a *luxS* mutant of enterohemorrhagic *Escherichia coli*. Infect. Immun. **75:**4875–4884.
25. **Lee, C. W., and M. L. Shuler.** 2000. The effect of inoculum density and conditioned medium on the production of ajmalicine and catharanthine from immobilized *Catharanthus roseus* cells. Biotechnol. Bioeng. **67:**61–71.
26. **Lenz, D. H., et al.** 2004. The small RNA chaperone Hfq and multiple small RNAs control quorum sensing in *Vibrio harveyi* and *Vibrio cholerae*. Cell **118:**69–82.
27. **Lewis, H. A., et al.** 2001. A structural genomics approach to the study of quorum sensing: crystal structures of three LuxS orthologs. Structure **9:**527–537.
28. **Li, J., et al.** 2007. Quorum sensing in *Escherichia coli* is signaled by AI-2/LsrR: effects on small RNA and biofilm architecture. J. Bacteriol. **189:**6011–6020.
29. **Li, J., et al.** 2006. A stochastic model of *Escherichia coli* AI-2 quorum signal circuit reveals alternative synthesis pathways. Mol. Syst. Biol. **2:**67.
30. **March, J. C., and W. E. Bentley.** 2004. Quorum sensing and bacterial cross-talk in biotechnology. Curr. Opin. Biotechnol. **15:**495–502.
31. **Neddermann, P., et al.** 2003. A novel, inducible, eukaryotic gene expression system based on the quorum-sensing transcription factor TraR. EMBO Rep. **4:**159–165.
32. **Ramirez, D. M., and W. E. Bentley.** 1995. Fed-batch feeding and induction policies that improve foreign protein synthesis and stability by avoiding stress responses. Biotechnol. Bioeng. **47:**596–608.
33. **Riesenberg, D., et al.** 1991. High cell-density cultivation of *Escherichia coli* at controlled specific growth rate. J. Biotechnol. **20:**17–28.
34. **Rodriguez, R. L., and R. C. Tait.** 1983. Recombinant DNA techniques: an introduction. Benjamin/Cummings Publishing Company, Inc., Menlo Park, CA.
35. **Salmond, G. P., B. W. Bycroft, G. S. Stewart, and P. Williams.** 1995. The bacterial "enigma": cracking the code of cell-cell communication. Mol. Microbiol. **16:**615–624.
36. **Sambrook, J., and D. W. Russell.** 2001. Molecular cloning: a laboratory manual, 3rd ed. Cold Spring Harbor Laboratory Press, Cold Spring Harbor, NY.
37. **Schauder, S., K. Shokat, M. G. Surette, and B. L. Bassler.** 2001. The LuxS family of bacterial autoinducers: biosynthesis of a novel quorum-sensing signal molecule. Mol. Microbiol. **41:**463–476.
38. **Schweder, T., et al.** 2002. Role of the general stress response during strong overexpression of a heterologous gene in *Escherichia coli*. Appl. Microbiol. Biotechnol. **58:**330–337.
39. **Srivastava, R., H. J. Cha, M. S. Peterson, and W. E. Bentley.** 2000. Antisense downregulation of σ^{32} as a transient metabolic controller in *Escherichia coli*: effects on yield of active organophosphorus hydrolase. Appl. Environ. Microbiol. **66:**4366–4371.
40. **Surette, M. G., and B. L. Bassler.** 1998. Quorum sensing in *Escherichia coli* and *Salmonella typhimurium*. Proc. Natl. Acad. Sci. U. S. A. **95:**7046–7050.
41. **Surette, M. G., M. B. Miller, and B. L. Bassler.** 1999. Quorum sensing in *Escherichia coli*, *Salmonella typhimurium*, and *Vibrio harveyi*: a new family of genes responsible for autoinducer production. Proc. Natl. Acad. Sci. U. S. A. **96:**1639–1644.
42. **Thomas, J. G., and F. Baneyx.** 1996. Protein folding in the cytoplasm of *Escherichia coli*: requirements for the DnaK-DnaJ-GrpE and GroEL-GroES molecular chaperone machines. Mol. Microbiol. **21:**1185–1196.
43. **Thomas, J. G., and F. Baneyx.** 1996. Protein misfolding and inclusion body formation in recombinant *Escherichia coli* cells overexpressing heat-shock proteins. J. Biol. Chem. **271:**11141–11147.
44. **Tjalsma, H., et al.** 2004. Engineering of quorum-sensing systems for improved production of alkaline protease by *Bacillus subtilis*. J. Appl. Microbiol. **96:**569–578.
45. **Tsao, C. Y., S. Hooshangi, H. C. Wu, J. J. Valdes, and W. E. Bentley.** 2010. Autonomous induction of recombinant proteins by minimally rewiring native quorum sensing regulon of *E. coli*. Metab. Eng. **12:**291–297.
46. **Vendeville, A., K. Winzer, K. Heurlier, C. M. Tang, and K. R. Hardie.** 2005. Making "sense" of metabolism: autoinducer-2, LuxS and pathogenic bacteria. Nat. Rev. Microbiol. **3:**383–396.
47. **Wang, L., Y. Hashimoto, C. Y. Tsao, J. J. Valdes, and W. E. Bentley.** 2005. Cyclic AMP (cAMP) and cAMP receptor protein influence both synthesis and uptake of extracellular autoinducer 2 in *Escherichia coli*. J. Bacteriol. **187:**2066–2076.
48. **Wang, L., J. Li, J. C. March, J. J. Valdes, and W. E. Bentley.** 2005. *luxS*-dependent gene regulation in *Escherichia coli* K-12 revealed by genomic expression profiling. J. Bacteriol. **187:**8350–8360.
49. **Weber, W., et al.** 2003. *Streptomyces*-derived quorum-sensing systems engineered for adjustable transgene expression in mammalian cells and mice. Nucleic Acids Res. **31:**e71.
50. **Wu, C. F., H. J. Cha, G. Rao, J. J. Valdes, and W. E. Bentley.** 2000. A green fluorescent protein fusion strategy for monitoring the expression, cellular location, and separation of biologically active organophosphorus hydrolase. Appl. Microbiol. Biotechnol. **54:**78–83.
51. **Xavier, K. B., and B. L. Bassler.** 2005. Regulation of uptake and processing of the quorum-sensing autoinducer AI-2 in *Escherichia coli*. J. Bacteriol. **187:**238–248.
52. **Zhu, J., R. Patel, and D. Pei.** 2004. Catalytic mechanism of S-ribosylhomocysteinase (LuxS): stereochemical course and kinetic isotope effect of proton transfer reactions. Biochemistry **43:**10166–10172.